

Lichen communities as a multiscale correlative indicator of elevational and land use-land cover gradients in the Himalayas

Himanshu Rai (✉ himanshurai08@yahoo.com)

Banaras Hindu University Department of Botany <https://orcid.org/0000-0001-8070-0602>

Roshni Khare

Savitribai Phule Pune University

Deepak Upadhyay

GB Pant Institute of Himalayan Environment and Development: Govind Ballabh Pant National Institute of Himalayan Environment and Sustainable Development

Rajan Kumar Gupta

Banaras Hindu University Department of Botany

Avinash B. Ade

Savitribai Phule Pune University

Samam Singh

IIRS: Indian Institute of Remote Sensing

Dalip Kumar Upreti

CSIR-National Botanical Research Institute

Research Article

Keywords: Himalaya, Land use- land cover, Lichens, Ordination, SRTM-DEM

Posted Date: November 23rd, 2021

DOI: <https://doi.org/10.21203/rs.3.rs-1100727/v1>

License:  This work is licensed under a Creative Commons Attribution 4.0 International License. [Read Full License](#)

Abstract

Elevation and land use/ land cover (LULC) plays an important role in the diversity of lichens in the Himalayas. The elevation gradients and LULC can be remotely assessed using remote sensing (RS) and geographical information systems (GIS). The current study was done in the Chopta-Tungnath landscape in the Kedarnath wildlife sanctuary, western Himalaya, India. Digital elevation modelling of the study area was done using shuttle radar topography mission data (SRTM-DEM) processed in Esri ArcGIS® ArcMAP™ 10.5, to assess the elevation gradient of the study area and selection of four lichen sampling sites. The LULC maps of the study area were prepared using Landsat 8 and Google Earth Pro 7.3.2.5776 imagery processed using Leica™ ERDAS IMAGINE® 9.2. An elevation gradient of 2750 m to 3703m was recorded by SRTM-DEM. The LULC analysis resulted in five LULC classes of which the four sampling sites fall in the 3 LULC classes. The principal component analysis (PCA), used to analyse the lichen communities along the RS-GIS recognized LULC classes. The study found lichen communities to be a proxy to the LULC classes in the Himalayas with clear gradients of growth forms and habitat subsets along the increasing elevation gradient.

Introduction

Studies on Lichens for the last few decades have been found them to be good indicators of land use in both managed as well as natural habitats reflecting the effects of both anthropogenic (i.e., habitat perturbations and pollution) and natural factors (i.e., invasive species, competition, and land-use intensity) (Pinho et al. 2012; Boch et al. 2016; Chuquimarca et al. 2019). Though there have been studies where remote sensing (RS) and geographical information systems (GIS) have been successfully used in assessing land use land cover (LULC) concerning dominant vegetation, their use for lichen diversity studies is still lacking (Prasad et al. 2015).

Among the various RS-GIS studies, Google Earth and Landsat data have been extensively used for LULC studies (Uddin et al. 2015; Debnath et al. 2017; Sharma et al. 2018; Mondal et al. 2019). The Google Earth imagery, an open-source data freely available has been instrumental for visual supervised classification of Landsat data and have been found efficient in the overall remote sensing classification of LULC (Tilahun and Teferie 2015; Uddin et al. 2015; Debnath et al. 2017; Sharma et al. 2018; Mondal et al. 2019).

In the present study, we have attempted digital elevational modelling of shuttle radar topography mission data in site selection and defining the elevation gradient of the Chopta-Tungnath landscape. The LULC estimation was done using Landsat-8 and Google earth data and their comparative efficiency was assessed. The above-mentioned RS-GIS analysis was correlated with the change in lichen diversity along with elevation and LULC changes to examine the capability of lichen communities as indicators of RS-GIS defined LULC in the mountainous terrain of Chopta-Tungnath landscape situated in the southern extreme of the Kedarnath wildlife sanctuary, western Himalaya.

Materials And Methods

3.1. Study area:

The study was conducted in the temperate-alpine habitats of Chopta-Tungnath (between 30°28'39"– 30°29'51" N latitude and 79°12'9" to 79°13'21" E longitude), a pasture and a trekking-pilgrimage area situated on the south-western fringe of Kedarnath wildlife sanctuary in the Garhwal Himalayas of Rudraprayag district, Uttarakhand (Figure 1A). The climate of the landscape is characterized by severe frost, diurnal to seasonal blizzards, hailstorms, and daily orographic precipitation at higher altitudes, throughout the year (Khare et al. 2010). The precipitation ensues in the form of snow, sleet-hail, rains, and showers throughout the year (Rai et al. 2012). The snowfall occurs from November to April. Snow melting in April is the major source of soil water before the monsoon. Maximum rainfall is recorded in July-August (Figure 1B). The mean monthly atmospheric temperature ranges from a maximum of 19°-37°C (May to October) to a minimum, as low as –15°C (December to February) (Figure 1B).

The area is known for the shrine of Tungnath, situated at the Tungnath ridge a major relief structure dividing the drainage of the region. The shrine is associated with alpine grassland (the Tungnath Bugyal). The Tungnath shrine lies 2 km below the Chandrashila Peak, the highest point of the landscape. The landscape is characterized by rocky outcrops having moderate to steep slopes. The topography of the area is dominated by ridges formed by exposed rocks and patches of flat temperate and alpine grasslands. The soil in the area is thin-layered, coarse-textured/ sandy loam at lower altitudes and sandy at higher altitudes, with proper drainage and acidic pH (pH 3.0-5.5) (Rai et al. 2012). The vascular plant vegetation of the study area shows stratified composition along the elevation gradient consisting of temperate mixed oak and coniferous forest at lower elevations, transitioning into the subalpine forest and ultimately culminating into alpine scrub/ grassland (Rai et al. 2012).

3.2. Remote sensing (RS) and geographical information systems (GIS) analysis:

3.2.1. Topographic studies using shuttle radar topography mission-digital elevation model (SRTM-DEM) data:

The topographic study of the Chopta-Tungnath landscape was done on shuttle radar topography mission-digital elevation model (SRTM-DEM) data. The SRTM was an international effort consisting of an 11-day mission of space shuttle Endeavour in February 2000, which mapped almost the entire earth from 56°S to 60°N with STRM payload employing interferometric synthetic-aperture radar technique and obtained a high-resolution digital topographical data of earth (Nikolakopoulos et al. 2006). SRTM-DEM data covers compiled by Consultative Group for International Agriculture Research Consortium for Spatial Information (CGIAR-CSI) covers about 80% of the globe. The SRTM 90m DEMs are with a resolution of 90m and are available for free download as 5×5-degree tiles at <http://srtm.csi.cgiar.org/>.

The 5×5-degree tile, SRTM, version 4, 90 m data of the study area was downloaded as Geo TIFF file from <http://srtm.csi.cgiar.org/srtmdata/> (Fig.2). The data file was pre-processed for noise reduction, identification, and elimination of man-made terrain features (if any), and for estimating and eliminating the forest canopy data (Köthe et al. 2009). The SRTM Geo TIFF file was processed in Esri ArcGIS® ArcMAP™ 10.5. The study area was clipped from the regional downloaded SRTM Geo TIFF file, using the shapefile created from Google Earth Pro 7.3.2.5776 (GEP). The processed SRTM data along with prior knowledge of the authors was used for the selection of probable sample areas. The final georeferenced and geotagged elevation map of the study area with sampling sites and landmarks was prepared using cumulative input data from SRTM-DEM, GEP, and previous field studies (Fig.2).

3.2.2. Land use land cover (LULC) classification:

The collative use of google earth imagery and Landsat data was done to assess and prepare the land use/ land cover of the study area (Fig. 4). The Google earth land use/land cover map was prepared by visual interpretation of data based on size, shape, tone, texture, association, and relationship to other objects (Fig. 4).

To study the Landsat-based land use/ land cover (LULC) of the study area, the Landsat 8 satellite data (path 145, row-39) of 18th February 2014 and 10th June 2014 was downloaded from the Earth Explorer website (<https://earthexplorer.usgs.gov/>). The satellite data was imported, stacked and the subset of area of interest (AOI) was created using Leica™ ERDAS IMAGINE® 9.2. The image was processed for preparing the unsupervised false-colour composite (FCC) map of the AOI using three bands (5, 4 and, 3), which was used in the field excursions for ground-truthing. For Google earth (GE) LULC studies the GE imagery of the Chopta-Tungnath landscape was downloaded using Google Earth Pro 7.3.2.5776 (GEP). The images were imported, stacked, noise reduction, image enhancement, and georeferencing were done as pre-processing (Fig. 3). The GEP imagery was processed for the preparation of the LULC map of AOI using 8 classification classes in Leica™ ERDAS IMAGINE® 9.2. The preliminary LULC maps i.e., FCC image by Landsat 8 and GEP LULC class maps were finally interpreted by supervised classification based on ground-truthing (Fig. 3).

Reconnaissance field visits/surveys were carried out in different months during 2014-2018 to establish the relationship between land use/ land cover and their tonal variation on the satellite data (Fig. 4). Ground truthing of the Landsat 8 FCC maps/ GEP LULC class maps was done using handheld GPS (Garmin GPSMAP® 76S).

The final land use/land cover (LULC) was interpreted using digital and visual analysis of Landsat 8 satellite/ GEP-LULC data. Supervised classification was performed with the training sites of known targets and then the spectral signatures of these sites were extrapolated to other unknown classes (Fig. 3). For this, the Gaussian maximum likelihood classification (GMLC) algorithm was used. The classifier used the training statistics to compute a probability value of whether it belongs to a particular class, which allows for the within-class spectral variance. In this image, the analyst used prior knowledge to weigh the probability function. GMLC provided the highest classification accuracies (Lillesand et al. 2015). For visual analysis elements of visual interpretation like tone, texture, shadow, was used to classify the land cover of the study area using Google Earth imagery and ground-truthing observations during field visits (Fig. 3). The LULC class area of each land use was calculated in km² and percent. The comparative error matrix and accuracy of visual (Google Earth Pro) and digital (Landsat 8, 2014) interpretation for the LULC classes were assessed using kappa index statistics and area measurements.

3.3. The quantitative study of lichen diversity:

3.3.1 Field methods, collection curation, and identification of lichens:

Based on the SRTM-DEM and previous field visit experiences of the two authors (i.e., Himanshu Rai and Roshni Khare), four sites of the collection were selected along the bridle approach path following the increasing elevation gradient from Chopta to Chandrashila through

Tungnath (Fig 4. Table 1). A circular plot of 24 m diam. was randomly selected at each site along the study landscape (Gasparyan et al. 2018; Nag et al. 2019). The lichen diversity was recorded employing a standardized probabilistic method with three 10×50 cm narrow frequency grids which were subdivided into five sampling units of 10×10 cm, laid randomly i.e., fifteen, 10×10 cm sampling units were laid in each plot (Asta et al. 2002; Scheidegger et al. 2002; Rai et al. 2012a, b; Nag et al. 2019). The lichen samples collected were air-dried and curated according to the standardized protocol (Obermayer 2002; Rai et al. 2014b).

The collected lichens were identified up to the species level at the Lichenology laboratory and herbarium (LWG) of the National Botanical Research Institute (NBRI), Lucknow, Uttar Pradesh, India using standardized morpho-anatomical examination, chemical spot tests, standardized thin-layer chromatography, and relevant literature (Awasthi 2007; Orange et al. 2010; Elix 2014; Rai et al. 2014b). The authenticated lichen samples were deposited as voucher specimens in the herbarium (LWG), NBRI.

3.4. Data analysis:

The lichen assemblage of all the four collection sites was quantitatively analyzed for frequency, regarding species richness (number of species) and growth form diversity, (Curtis and McIntosh 1950; Rai et al. 2012). The indirect gradient ordination method, principal component analysis (PCA), was used to summarise the compositional differences of lichen communities between the sites using the var-covariance matrix, employing singular value decomposition, along the RS-GIS recognized LULC classes (Gauch 1982; Ter Braak 1995; Ter Braak and Prentice 2004; Rai et al. 2012).

Results

4.1. Remote sensing (RS) and geographical information systems (GIS) analysis:

The SRTM-DEM obtained with a pixel size of 90 m covered a total area of 10.25 km² with elevational variation ranging from 2750 m to 3703m (Fig. 5). The collative LULC studies using Landsat 8, FCC, and Google Earth imagery identified five LULC classes (Table 2, Fig 6). Among the identified LULC classes the mixed conifer forest dominated followed by temperate grassland, Rhododendron sub-alpine forests, alpine grassland, and snow (Table 2). The accuracy assessment found the LULC classes derived by the visual interpretation using Google Earth Pro imagery to be more efficient than the LULC classes derived by the digital classification using Landsat 8, 2014 data (Table 3). The reconnaissance field visits/ surveys carried out during the study period (i.e., 2014-2018) further observed stratification of vegetation along increasing elevational gradients in the landscape. The LULC classes identified through RS-GIS studies were defined by these vegetational stratifications. The mixed conifer forests were dominated by strands of *Quercus semecarpifolia* and *Rhododendron arboreum* with few patches of *Abies pindrow* and *Taxus baccata* trees (Fig. 7). The temperate grasslands developed in the open canopy area in the coniferous forests (Fig. 7). The Rhododendron sub-alpine forests entirely consisted of coppices of *Rhododendron campanulatum* (Fig. 7). The alpine grassland was dominated by the vegetation of herb species of *Anemone*, *Potentilla*, *Aster*, *Geranium*, *Meconopsis*, *Primula*, and *Polemonium*, with scattered patches of shrubs of *Rhododendron anthopogon* and *Juniperus* species (Fig. 7).

4.2. Average lichen community structure, patterns.

The lichen assemblage recorded from the four sites in the Chopta–Tungnath landscape consisted of 104 species belonging to 28 genera, 11 families, and four growth forms (Table 4). Among the lichen families, Parmaliaceae (37 species) dominated followed by Physciaceae (14 species), Cladoniaceae (12 species), Stereocaulaceae (8 species), Collamatceae, Peltigeraceae, and Ramalinaceae (6 species each), Umbilicariaceae (2 species), and Nephromataceae (1 species) (Table 4). Among the various growth forms of lichen recorded leafy foliose (65 species) dominated followed by compound (18 species)-having squamules as primary thallus bearing erect fruticose body as the secondary thallus, fruticose (14 species), and powdery leprose (3 species) (Table 4). The number of lichen species recorded was maximum in site 1 (i.e., 50 species) followed by site 2 (19 species), site 3 (14 species), and site 4 (12 species). The lichen habitat-subsets show a striking gradient where the bark inhabiting corticolous lichen species dominated in sites 1 and 2 gradually replaced by more dominant soil-inhabiting terricolous lichen species in sites 3 and 4 (Fig. 8A). Among the growth forms, the foliose lichens were present throughout the landscape, the more complex compound growth forms increased along with increasing elevation gradients (Fig. 8B)

4.3. Lichen communities and RS-GIS defined LULC classes:

The PCA analysis required 3 components (axis) to account for a 100% variation in the data set. The first two axes of PCA explained 87.2% of the variance, and each axis explained 69.6 and 16.6 % of the variance, respectively (Fig.9). Sites 1 and 2 mapped separately whereas sites 3 and 4 mapped coherently due to their inherent similarity and differences in the diversity of constituent lichen species at

each site (Fig. 9). The PCA biplot further concluded that the lichen community at site 1 was indicative of the RS-GIS recognized LULC class mixed conifer forest, whereas site 2 of *Rhododendron* sub-alpine forest and sites 3 and 4 of alpine grassland (Fig. 9).

Discussion

The Himalayan vegetation is highly influenced by climatic, elevational, geological, topographical, and anthropogenic parameters (Singh and Singh 1987). Lichens are among some of the organisms which exhibit substantial distribution throughout the Himalayan landscapes with diverse growth forms inhabiting all the terrestrial domains (Upreti 1987). The LULC types recognized using Landsat-8 and Google earth imagery gives a more distinguished forest cover estimation than already known of the area (Rai et al. 2012, 2014). The presence of temperate grasslands in the open canopy regions of the mixed coniferous forests is more prominent in the LULC maps prepared by the RS-GIS data (Rai et al. 2012, 2014). The change in both quantitative (i.e., the number of species, quadrat frequency of the lichen species) and qualitative (growth forms, habitat subsets) diversity along the LULC and the elevational gradient is per previous studies done on terricolous lichen communities (Rai et al. 2012, 2014). The higher species diversity in low elevation-mixed conifer forests is due to the presence of tree barks of the phorophytes (*Quercus* spp., *Rhododendron* spp., *Abies* spp. and *Taxus* spp.) as preferred substratum, which fades out at higher elevation where the tree line diminishes and is replaced by alpine grasslands having soil/ ground and rocks the only substratum available for the lichens to colonize (Negi 2000; Rai et al. 2012, 2014). The PCA analysis establishes that the lichen communities are indicative of RS-GIS-recognized LULC classes, which harbour different combinations of lichen growth forms and habitat subsets guided by the LULC classes. The overall efficient recognition of LULC classes by Google earth imagery over Landsat-8 data is because the GEPr program prepares maps by superimposing satellite images, aerial photography, and GIS data making the output maps more accurate.

Conclusion

The study hereby elucidates the influence of LULC on the lichen communities along the elevation gradient of the Chopta-Tungnath landscape. The efficiency of GEPr-LULC mapping over Landsat 8-FCC indicates their superior remote sensing LULC analytic applications. The clustering of lichen communities to specific LULC with defined combinations of growth forms and habitat subsets, concludes their ability and probable applications as indicators of different vegetational covers and land use in the Himalaya. The findings can be used for developing forest management policies and can be of considerable help for biodiversity assessment in the Himalayas.

Declarations

Acknowledgments Authors are grateful to the Director, CSIR-National Botanical Research Institute, Lucknow for providing necessary laboratory facilities. The work of Himanshu Rai was supported by the Uttarakhand State Council for Science and Technology, through the MRD project grant (UCOST-UCS&T/R&D/LS-26/11-12/4370 dated 17-03-2012).

References

1. Asta J, Erhardt W, Ferretti M, Fornasier F, Kirschbaum U, Nimis PL, Purvis OW, Pirintsos S, Scheidegger C, Van Haluwyn C, Wirth V (2002) Mapping Lichen Diversity as an Indicator of Environmental Quality.. In: Nimis PL, Scheidegger C, Wolseley PA (eds) Monitoring with Lichens – Monitoring Lichens. Springer, Dordrecht, pp 273–279. https://doi.org/10.1007/978-94-010-0423-7_19
2. Awasthi DD (2007) A compendium of the macrolichens from India, Nepal, and Sri Lanka. Bishen Singh Mahendra Pal Singh, Dehra Dun
3. Boch S, Prati D, Schöning I, Fischer M (2016) Lichen species richness is highest in non-intensively used grasslands promoting suitable microhabitats and low vascular plant competition. *Biodivers Conserv* 25:225–238. <https://doi.org/10.1007/s10531-015-1037-y>
4. Chuquimarca L, Gaona FP, Iñiguez-Armijos C, Benítez Á (2019) Lichen Responses to Disturbance: Clues for Biomonitoring Land-use Effects on Riparian Andean Ecosystems. *Diversity* 11:73. <https://doi.org/10.3390/d11050073>
5. Curtis JT, McIntosh RP (1950) The Interrelations of Certain Analytic and Synthetic Phytosociological Characters. *Ecology* 31:434–455. <https://doi.org/10.2307/1931497>
6. Debnath J, Das N, Ahmed I, Bhowmik M (2017) Channel migration and its impact on land use/land cover using RS and GIS: A study on Khowai River of Tripura, North-East India. *The Egyptian Journal of Remote Sensing and Space Science* 20:197–210. <https://doi.org/10.1016/j.ejrs.2017.01.009>

7. Elix JA (2014) A catalogue of standardized thin layer chromatographic data and biosynthetic relationships for lichen substances, 3rd edn. Australian National University, Canberra, Australia. <https://www.anbg.gov.au/abrs/lichenlist/Chem%20Cat%203.pdf> Accessed on 15 Nov 2019.
8. Gasparyan A, Sipman HJM, Marini L, Nascimbene J (2018) The inclusion of overlooked lichen microhabitats in standardized forest biodiversity monitoring. *The Lichenologist* 50:231–237. <http://dx.doi.org/10.1017/S0024282918000087>
9. Gauch HG (1982) *Multivariate Analysis in Community Ecology*. Cambridge University Press, Cambridge. <https://doi.org/10.1017/CBO9780511623332>
10. Khare R, Rai H, Upreti DK, Gupta RK, Plants, Pollution E, Lucknow CSIR-NBRI (2010) U.P, 8-11 Dec, pp.135-136. <http://dx.doi.org/10.13140/2.1.1812.5604>
11. Köthe R, Bock M (2009) Preprocessing of digital elevation models–derived from laser scanning and radar interferometry–for terrain analysis in geosciences. *Proceedings of geomorphometry, Zurich, Switzerland*, 31
12. Mondal T, Basu P, Qureshi Q, Jhala Y (2019) An assessment of land use land cover change in Central Highland of Deccan Peninsula and Semi-Arid tracts of India. *bioRxiv*, 665794. <https://doi.org/10.1101/665794>
13. Nag P, Gupta RK, Upreti DK (2019) Lichenized fungi *Stereocaulon foliolosum* Nyl. (Stereocaulaceae, Ascomycota), indicator of ambient air metal deposition in a temperate habitat of Kumaun, central Himalaya, India. *Tropical Plant Research* 6:199–205. <https://doi.org/10.22271/tpr.2019.v6.i2.029>
14. Negi HR (2000) On the patterns of abundance and diversity of macrolichens of Chopta-Tunganath in the Garhwal Himalaya. *J Biosci* 25:367–378. doi: <http://dx.doi.org/10.1007/BF02703790>
15. Nikolakopoulos KG, Kamaratakis EK, Chrysoulakis N (2006) SRTM vs ASTER elevation products. Comparison for two regions in Crete, Greece. *Int J Remote Sens* 27:4819–4838. <http://dx.doi.org/10.1080/01431160600835853>
16. Obermayer W (2002) Management of a Lichen Herbarium.. In: In: Kranner IC, Beckett RP, Varma AK (eds) *Protocols in Lichenology: Culturing, Biochemistry, Ecophysiology and Use in Biomonitoring*. Springer, Berlin Heidelberg, pp 507–523. https://doi.org/10.1007/978-3-642-56359-1_29
17. Orange A, James PW, White FJ (2001) *Microchemical methods for the identification of lichens*. British Lichen Society, London
18. Pinho P, Bergamini A, Carvalho P, Branquinho C, Stofer S, Scheidegger C, Máguas C (2012) Lichen functional groups as ecological indicators of the effects of land-use in Mediterranean ecosystems. *Ecol Ind* 15:36–42. <https://doi.org/10.1016/j.ecolind.2011.09.022>
19. Prasad N, Semwal M, Roy PS (2015) *Remote Sensing and GIS for Biodiversity Conservation*.. In: In: Upreti DK, Divakar PK, Shukla V, Bajpai R (eds) *Recent Advances in Lichenology: Modern Methods and Approaches in Biomonitoring and Bioprospection*, vol 1. Springer India, New Delhi, pp 151–179. https://doi.org/10.1007/978-81-322-2181-4_7
20. Rai H, Gupta RK, Upreti DK, Nag P (2014) Distribution Pattern of Terricolous Lichens in Garhwal Himalayas (Chopta-Tungnath Tract) with Reference to Morphological and Environmental Variables. In: Gupta RK, Kumar M (eds) *Diversity of Lower Plants*, I.K. International Publisher, New Delhi, India, pp 264-278. <http://dx.doi.org/10.13140/2.1.3237.9689>
21. Rai H, Khare R, Gupta RK, Upreti DK (2012a) Terricolous lichens as indicator of anthropogenic disturbances in a high altitude grassland in Garhwal (Western Himalaya), India. *Botanica Orientalis* 8:16–23. <https://doi.org/10.3126/botor.v8i0.5554>
22. Rai H, Khare R, Upreti DK, Ahti T (2014a) Terricolous Lichens of India: Taxonomic Keys and Description.. In: In: Rai H, Upreti DK (eds) *Terricolous Lichens in India: Volume 2: Morphotaxonomic Studies*. Springer New York, New York, NY, pp 17–294. https://doi.org/10.1007/978-1-4939-0360-3_2
23. Rai H, Khare R, Upreti DK, Nayaka S (2014b) Terricolous Lichens of India: An Introduction to Field Collection and Taxonomic Investigations. In: Rai H, Upreti DK (eds) *Terricolous Lichens in India: Volume 2: Morphotaxonomic Studies*. Springer New York, pp 1-16. https://doi.org/10.1007/978-1-4939-0360-3_1
24. Rai H, Upreti DK, Gupta RK (2012b) Diversity and distribution of terricolous lichens as indicator of habitat heterogeneity and grazing induced trampling in a temperate-alpine shrub and meadow. *Biodivers Conserv* 21:97–113. <http://dx.doi.org/10.1007/s10531-011-0168-z>
25. Scheidegger C, Groner U, Keller C, Stofer S (2002) Biodiversity Assessment Tools – Lichens.. In: In: Nimis PL, Scheidegger C, Wolseley PA (eds) *Monitoring with Lichens-Monitoring Lichens*. Springer, Netherlands, pp 359–365. https://doi.org/10.1007/978-94-010-0423-7_35
26. Sharma J, Prasad R, Mishra VN, Yadav VP, Bala R (2018) Land Use and Land Cover Classification of Multispectral LANDSAT-8 Satellite Imagery Using Discrete Wavelet Transform. *International Archives of the Photogrammetry, Remote Sensing and Spatial Information Sciences* 42:5. <https://doi.org/10.5194/isprs-archives-XLII-5-703-2018>

27. Singh JS, Singh SP (1987) Forest vegetation of the Himalaya. *The Botanical Review* 53:80–192. <https://doi.org/10.1007/BF02858183>
28. Ter Braak CJF (1995) Ordination.. In: In: Ter Braak CJF, Van Tongeren OFR, Jongman RHG (eds) *Data Analysis in Community and Landscape Ecology*. Cambridge University Press, Cambridge, pp 91–173. <https://doi.org/10.1017/CBO9780511525575.007>
29. Ter Braak CJF, Prentice IC (2004) A Theory of Gradient Analysis. *Adv Ecol Res* 34:235–282. [https://doi.org/10.1016/S0065-2504\(03\)34003-6](https://doi.org/10.1016/S0065-2504(03)34003-6)
30. Tilahun A, Teferie B (2015) Accuracy assessment of land use land cover classification using Google Earth. *American Journal of Environmental Protection* 4:193–198. <https://doi.org/10.11648/j.ajep.20150404.14>
31. Uddin K, Chaudhary S, Chettri N, Kotru R, Murthy M, Chaudhary RP, Ning W, Shrestha SM, Gautam SK (2015) The changing land cover and fragmenting forest on the Roof of the World: A case study in Nepal's Kailash Sacred Landscape. *Landscape and Urban Planning* 141:1–10. <https://doi.org/10.1016/j.landurbplan.2015.04.003>
32. Upreti DK (1998) Diversity of lichens in India.. In: In: Agarwal SK, Kaushik JP, Kaul KK, Jain AK (eds) *Perspectives in environment*. APH Publishing Corporation, New Delhi, pp 71–79

Tables

Table 1: Geo-attributes, of the four collection sites and prominent landmarks of Chopta-Tungnath, Kedarnath wildlife sanctuary, western Himalaya

Landmarks/ collection sites	Coordinates	Average elevation (m)
Chopta chatti	N 30 ⁰ 29' 05.8" E 79 ⁰ 11' 59.7"	2838
Site 1	N 30 ⁰ 29' 12.03" E 79 ⁰ 12' 05.3"	2990
Site 2	N 30 ⁰ 29' 18.3" E 79 ⁰ 12' 31.3"	3236
Site 3	N 30 ⁰ 29' 18.2" E 79 ⁰ 12' 60.0"	3442
Site 4	N 30 ⁰ 29' 12.7" E 79 ⁰ 13' 16.4"	3668
Tungnath temple complex	N 30 ⁰ 29' 17.8" E 79 ⁰ 13' 01.1"	3640
Chandrashila	N 30 ⁰ 29' 13.1" E 79 ⁰ 13' 18.2"	3672

Table 2: The land use land cover (LULC) area of the visual (Google Earth Pro) and digital-supervised (Landsat 8, 2014) classification of the study landscape (Chopta-Tungnath)

SNo.	LULC classes	Visual classification area (km ²)	Area (%)	Digital-supervised classification area (km ²)	Area (%)
1.	Mixed conifer forest	5.31	51.81	4.90	47.80
2.	Temperate grassland	2.44	23.80	3.40	33.17
3.	Rhododendron sub-alpine forest	0.14	1.37	0.25	2.44
4.	Alpine grassland	2.17	21.17	1.55	15.12
5.	Snow	0.19	1.85	0.15	1.56
	Total area	10.25		10.25	

Table 3: Error matrix and accuracy of visual (Google Earth Pro) and digital (Landsat 8, 2014) interpretation for the land use land cover (LULC) classes of the study landscape (Chopta-Tungnath)

SNo.	LULC classes	Digital Interpretation (Landsat 8, 2014)		Visual interpretation (Google Earth Pro)	
		Producer accuracy	User accuracy	Producer accuracy	User accuracy
1.	Mixed conifer forest	81.82	81.82	89.47	89.47
2.	Temperate grassland	87.50	93.33	100.00	90.91
3.	Rhododendron sub-alpine forest	100.00	100.00	100.00	100.00
4.	Alpine grassland	40.00	40.00	81.82	90.00
5.	Snow	100.00	92.86	100.00	100.00
	Overall accuracy	86.00		92.00	
	Kappa coefficient	0.8165		0.8930	

Table 4: Lichens and their quantitative diversity (quadrate frequency) recorded in the four sites of the three RS- GIS recognised LULC types of the Chopta-Tungnath landscape

SNo.	Lichen Species	Family	Growth form	Elevation (m)	Site 1			Site 2			Site 3			Site 4		
					Cr	Sx	Tr	Cr	Sx	Tr	Cr	Sx	Tr	Cr	Sx	Tr
1.	<i>Bryoria confusa</i>	Parmeliaceae	Fo	3321	-	-	-	6.7	-	26.7	-	-	-	-	-	-
2.	<i>Bulbothrix setschwanensis</i>	Parmeliaceae	Fo	2967	33.3	-	-	-	-	-	-	-	-	-	-	-
3.	<i>Cetrelia olivetorum</i>	Parmeliaceae	Fo	2995	-	-	33.3	-	-	-	-	-	-	-	-	-
4.	<i>Cetreliaopsis rhytidocarpa</i>	Parmeliaceae	Fo	2992	33.3	-	-	-	-	-	-	-	-	-	-	-
5.	<i>Cladonia cartilaginea</i>	Cladoniaceae	Cd	3384	-	-	-	-	-	-	-	-	33.3	-	-	-
6.	<i>Cladonia ceratophyllina</i>	Cladoniaceae	Cd	3558	-	-	-	-	-	-	-	-	33.3	-	-	-
7.	<i>Cladonia chlorophaea</i>	Cladoniaceae	Cd	3226	-	-	-	-	-	-	-	-	33.3	-	-	-
8.	<i>Cladonia coccifera</i>	Cladoniaceae	Cd	3225	-	-	-	-	-	-	6.7	26.7	-	-	-	-
9.	<i>Cladonia coccifera</i>	Cladoniaceae	Cd	3446	-	-	-	-	-	-	-	-	-	-	-	86.7
10.	<i>Cladonia coniocraea</i>	Cladoniaceae	Cd	2970	6.7	-	66.7	-	-	-	-	-	-	-	-	-
11.	<i>Cladonia fimbriata</i>	Cladoniaceae	Cd	3356	-	-	-	-	-	-	-	-	33.3	-	-	-
12.	<i>Cladonia furcata</i>	Cladoniaceae	Cd	3248	-	-	-	-	-	-	-	-	33.3	-	-	-
13.	<i>Cladonia pyxidata</i>	Cladoniaceae	Cd	3356	-	-	-	-	-	-	-	-	-	-	-	33.3
14.	<i>Cladonia ramulosa</i>	Cladoniaceae	Cd	2991	-	-	80	-	-	-	-	-	-	-	-	-
15.	<i>Cladonia scabriuscula</i>	Cladoniaceae	Cd	3130	-	-	66.7	-	-	-	-	-	-	-	-	-
16.	<i>Cladonia subulata</i>	Cladoniaceae	Cd	2943	-	-	66.7	-	-	-	-	-	-	-	-	-
17.	<i>Dermatocarpon miniatum</i>	Verrucariaceae	Fo	3131	-	46.7	-	-	-	-	-	-	-	-	-	-
18.	<i>Dermatocarpon velleum</i>	Verrucariaceae	Fo	35-4	-	-	-	-	-	-	-	-	-	-	33.3	-
19.	<i>Everniastrum cirrhatum</i>	Parmeliaceae	Fo	2966	80	-	-	-	-	-	-	-	-	-	-	-
20.	<i>Everniastrum nepalense</i>	Parmeliaceae	Fo	2942	73.3	-	-	-	-	-	-	-	-	-	-	-
21.	<i>Flavopunctelia soledica</i>	Parmeliaceae	Fo	2967	40	-	-	-	-	-	-	-	-	-	-	-
23.	<i>Heterodermia angustiloba</i>	Physciaceae	Fo	3272	-	-	-	33.3	-	-	-	-	-	-	-	-
24.	<i>Heterodermia boryi</i>	Physciaceae	Fo	2953	46.7	-	-	-	-	-	-	-	-	-	-	-
25.	<i>Heterodermia comosa</i>	Physciaceae	Fo	2946	13.3	-	-	-	-	-	-	-	-	-	-	-
26.	<i>Heterodermia diademata</i>	Physciaceae	Fo	2971	40	46.7	-	-	-	-	-	-	-	-	-	-
27.	<i>Heterodermia dissecta</i> var. <i>koyana</i>	Physciaceae	Fo	2979	26.7	13.3	-	-	-	-	-	-	-	-	-	-
28.	<i>Heterodermia hypocaustia</i>	Physciaceae	Fo	3250	-	-	-	13.3	-	20	-	-	-	-	-	-
29.	<i>Heterodermia incana</i>	Physciaceae	Fo	2989	33.3	-	-	-	-	-	-	-	-	-	-	-
30.	<i>Heterodermia obscurata</i>	Physciaceae	Fo	3652	-	-	-	-	-	-	-	-	-	-	-	26.7
31.	<i>Heterodermia pseudospeciosa</i>	Physciaceae	Fo	2998	-	33.3	-	-	-	-	-	-	-	-	-	-
32.	<i>Heterodermia pseudospeciosa</i>	Physciaceae	Fo	3209	-	-	-	-	33.3	6.7	-	-	-	-	-	-
33.	<i>Heterodermia punctifera</i>	Physciaceae	Fo	3343	-	-	-	6.7	26.7	-	-	-	-	-	-	-
34.	<i>Hypotrachyna adducta</i>	Parmeliaceae	Fo	2930	6.7	-	-	-	-	-	-	-	-	-	-	-
35.	<i>Hypotrachyna awasthii</i>	Parmeliaceae	Fo	3253	-	-	-	33.3	-	-	-	-	-	-	-	-
36.	<i>Hypotrachyna crenata</i>	Parmeliaceae	Fo	2994	26.7	3.3	3.3	-	-	-	-	-	-	-	-	-
37.	<i>Hypotrachyna</i>	Parmeliaceae	Fo	2925	13.3	-	-	-	-	-	-	-	-	-	-	-

38.	<i>physcioides</i> <i>Hypotrachyna</i> <i>pindarensis</i>	Parmeliaceae	Fo	3456	-	-	-	-	-	-	-	-	-	-	33.3	-
39.	<i>Hypotrachyna</i> <i>pseudo-sinuosa</i>	Parmeliaceae	Fo	3548	-	-	-	-	-	-	-	-	-	33.3	-	-
40.	<i>Lepraria</i> <i>caesioalba</i> var. <i>groenlandica</i>	Stereocaulaceae	Lp	2991	-	-	33.3	-	-	-	-	-	-	-	-	-
41.	<i>Lepraria neglecta</i>	Stereocaulaceae	Lp	2926	6.7	6.7	40	-	-	-	-	-	-	-	-	-
42.	<i>Leptogium</i> <i>askotense</i>	Collemataceae	Fo	3442	-	-	-	-	-	-	6.7	6.7	20	-	-	-
43.	<i>Leptogium</i> <i>burnetiae</i>	Collemataceae	Fo	3237	-	-	-	26.7	13.3	-	-	-	-	-	-	-
44.	<i>Leptogium delavayi</i>	Collemataceae	Fo	3546	-	-	-	-	-	-	-	-	-	6.7	-	33.3
45.	<i>Leptogium</i> <i>javanicum</i>	Collemataceae	Fo	3358	-	-	-	-	-	-	13.3	-	20	-	-	-
46.	<i>Leptogium</i> <i>pedicellatum</i>	Collemataceae	Fo	2987	33.3	-	66.7	-	-	-	-	-	-	-	-	-
47.	<i>Leptogium</i> <i>trichophorum</i>	Collemataceae	Fo	3254	-	-	-	13.3	-	20	-	-	-	-	-	-
48.	<i>Lobaria isidiosa</i>	Lobariaceae	Fo	2996	33.3	-	-	-	-	-	-	-	-	-	-	-
49.	<i>Lobaria</i> <i>kurokawae</i>	Lobariaceae	Fo	2991	-	-	33.3	-	-	-	-	-	-	-	-	-
50.	<i>Lobaria retigera</i>	Lobariaceae	Fo	3248	-	-	-	-	-	-	-	6.7	26.7	-	-	-
51.	<i>Melanelia stygia</i>	Parmeliaceae	Fo	3400	-	-	-	-	-	-	-	-	-	-	20	13.3
52.	<i>Myelochroa</i> <i>entotheiochroa</i>	Parmeliaceae	Fo	2994	33.3	-	-	-	-	-	-	-	-	-	-	-
53.	<i>Myelochroa</i> <i>perisidians</i>	Parmeliaceae	Fo	2994	33.3	-	-	-	-	-	-	-	-	-	-	-
54.	<i>Nephroma</i> <i>helveticum</i>	Nephromataceae	Fo	2947	26.7	-	-	-	-	-	-	-	-	-	-	-
55.	<i>Parmelia</i> <i>meiophora</i>	Parmeliaceae	Fo	3227	-	-	-	33.3	-	-	-	-	-	-	-	-
56.	<i>Parmelia saxatilis</i>	Parmeliaceae	Fo	3307	-	-	-	13.3	20	-	-	-	-	-	-	-
57.	<i>Parmelia sulcata</i>	Parmeliaceae	Fo	3228	-	-	-	33.3	-	-	-	-	-	-	-	-
58.	<i>Parmelinella</i> <i>simplicior</i>	Parmeliaceae	Fo	2979	46.7	-	-	-	-	-	-	-	-	-	-	-
59.	<i>Parmelinella</i> <i>wallichiana</i>	Parmeliaceae	Fo	2942	46.7	-	-	-	-	-	-	-	-	-	-	-
60.	<i>Parmotrema</i> <i>andinum</i>	Parmeliaceae	Fo	2938	6.7	26.7	-	-	-	-	-	-	-	-	-	-
61.	<i>Parmotrema</i> <i>nilgherrense</i>	Parmeliaceae	Fo	2993	26.7	-	-	-	-	-	-	-	-	-	-	-
62.	<i>Parmotrema</i> <i>reticulatum</i>	Parmeliaceae	Fo	2952	53.3	-	-	-	-	-	-	-	-	-	-	-
63.	<i>Parmotrema</i> <i>robustum</i>	Parmeliaceae	Fo	3139	-	-	-	33.3	-	-	-	-	-	-	-	-
64.	<i>Parmotrema</i> <i>saccatilobum</i>	Parmeliaceae	Fo	2991	33.3	-	-	-	-	-	-	-	-	-	-	-
65.	<i>Parmotrema</i> <i>tinctorum</i>	Parmeliaceae	Fo	2959	-	33.3	-	-	-	-	-	-	-	-	-	-
66.	<i>Peltigera canina</i>	Peltigeraceae	Fo	3445	-	-	-	-	-	-	-	-	33.3	-	-	-
67.	<i>Peltigera</i> <i>dolichorrhiza</i>	Peltigeraceae	Fo	3456	-	-	-	-	-	-	6.7	6.7	20	-	-	-
68.	<i>Peltigera</i> <i>praetextata</i>	Peltigeraceae	Fo	3444	-	-	-	-	-	-	-	-	33.3	-	-	-
69.	<i>Peltigera</i> <i>rufescens</i>	Peltigeraceae	Fo	3205	-	-	-	-	-	-	-	-	33.3	-	-	-
70.	<i>Phaeophyscia</i> <i>endococcina</i>	Physciaceae	Fo	2944	40	-	-	-	-	-	-	-	-	-	-	-
71.	<i>Phaeophyscia</i> <i>hispidula</i>	Physciaceae	Fo	2988	53.3	-	-	-	-	-	-	-	-	-	-	-
72.	<i>Physconia grisea</i>	Physciaceae	Fo	3652	-	-	-	-	-	-	-	-	-	-	-	33.3
73.	<i>Punctelia rudecta</i>	Parmeliaceae	Fo	3303	-	-	-	33.3	-	-	-	-	-	-	-	-
74.	<i>Ramalina</i> <i>himalayensis</i>	Ramalinaceae	Fr	3402	-	-	-	-	-	-	26.7	6.7	-	-	-	-
75.	<i>Ramalina hossei</i>	Ramalinaceae	Fr	2938	33.3	-	13.3	-	-	-	-	-	-	-	-	-
76.	<i>Ramalina roesleri</i>	Ramalinaceae	Fr	2944	20	-	-	-	-	-	-	-	-	-	-	-

78.	<i>Ramalina sinensis</i>	Ramalinaceae	Fr	2950	33.3	-	-	-	-	-	-	-	-	-	-
79.	<i>Stereocaulon alpinum</i>	Stereocaulaceae	Cd	3344	-	-	-	6.7	26.7	-	-	-	-	-	-
80.	<i>Stereocaulon foliolosum</i>	Stereocaulaceae	Cd	3350	-	-	-	6.7	26.7	-	-	-	-	-	-
81.	<i>Stereocaulon foliolosum var strictum</i>	Stereocaulaceae	Cd	3253	-	-	-	6.7	26.7	-	-	-	-	-	-
82.	<i>Stereocaulon macrocephalum</i>	Stereocaulaceae	Cd	3486	-	-	-	-	-	-	-	-	6.7	26.7	
83.	<i>Stereocaulon massartianum</i>	Stereocaulaceae	Cd	2957	-	-	33.3	-	-	-	-	-	-	-	
84.	<i>Stereocaulon pomiferum</i>	Stereocaulaceae	Cd	2936	-	-	66.7	-	-	-	-	-	-	-	
85.	<i>Sticta henryana</i>	Lobariaceae	Fo	2944	6.7	-	-	-	-	-	-	-	-	-	
86.	<i>Umbilicaria indica var. nana</i>	Umbilicariaceae	Fo	3252	-	-	-	33.3	-	-	-	-	-	-	
87.	<i>Umbilicaria vellea</i>	Umbilicariaceae	Fo	3645	-	-	-	-	-	-	-	-	33.3	-	
88.	<i>Usnea baileyi</i>	Parmeliaceae	Fr	3391	-	-	-	33.3	-	-	-	-	-	-	
89.	<i>Usnea himalayana</i>	Parmeliaceae	Fr	3179	-	-	-	33.3	-	-	-	-	-	-	
90.	<i>Usnea longissima</i>	Parmeliaceae	Fr	3542	-	-	-	-	-	-	-	-	-	33.3	
99.	<i>Usnea orientalis</i>	Parmeliaceae	Fr	2927	33.3	-	-	-	-	-	-	-	-	-	
100.	<i>Usnea perplexans</i>	Parmeliaceae	Fr	2949	73.3	-	-	-	-	-	-	-	-	-	
101.	<i>Usnea pseudosinensis</i>	Parmeliaceae	Fr	2971	33.3	-	-	-	-	-	-	-	-	-	
102.	<i>Usnea stigmatoides</i>	Parmeliaceae	Fr	2949	13.3	-	-	-	-	-	-	-	-	-	
103.	<i>Usnea subfloridana</i>	Parmeliaceae	Fr	2927	6.7	-	-	-	-	-	-	-	-	-	
104.	<i>Usnea eumitrioides</i>	Parmeliaceae	Fr	2903	33.3	-	-	-	-	-	-	-	-	-	

Growth forms, Lp leprose, Fo foliose, Fr fruticose, Cd compound; Substrate subsets, Cr corticolous (on bark), Sx saxicolous (on rock), Tr terricolous (on soil)

Figures

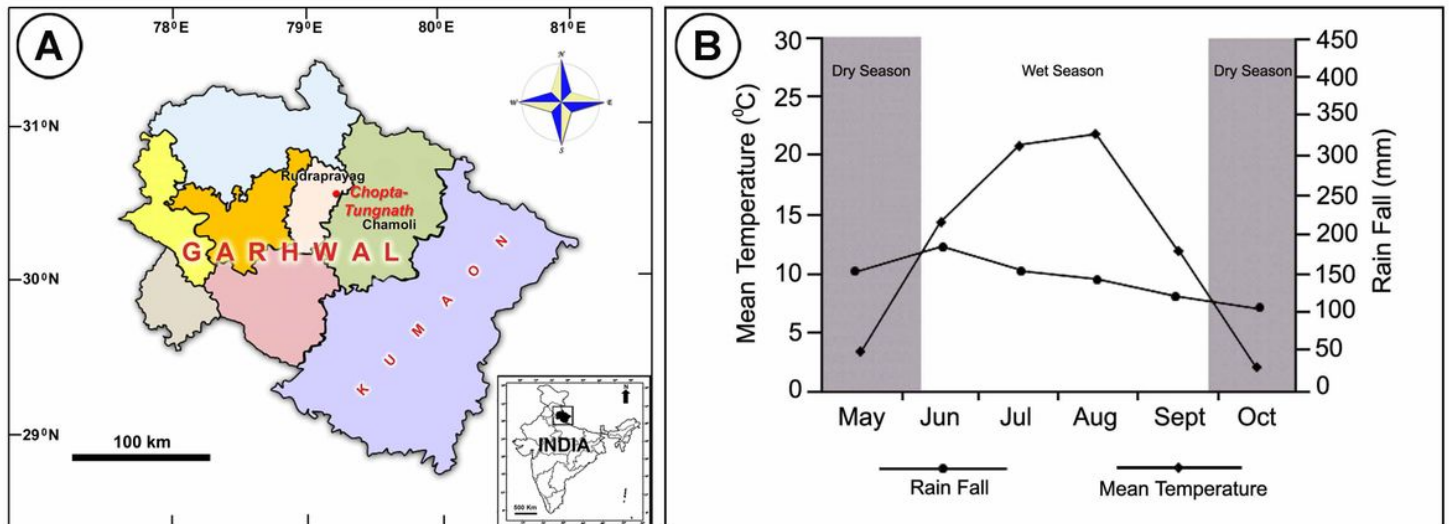


Figure 1

A, the location map of the study area, B, the pluviothermic diagram showing wet and dry months in Chopta- Tungnath landscape (redrawn after Rai et al. 2012a)

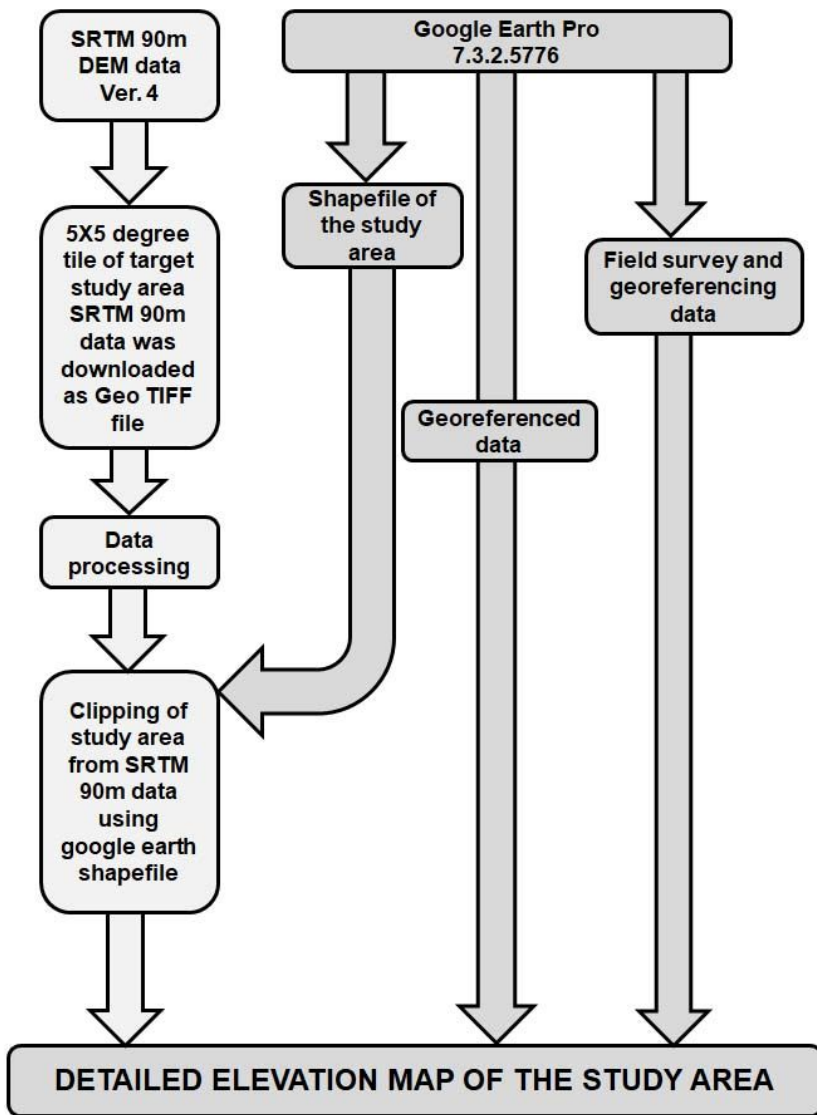


Figure 2

An overview of SRTM-DEM analysis.

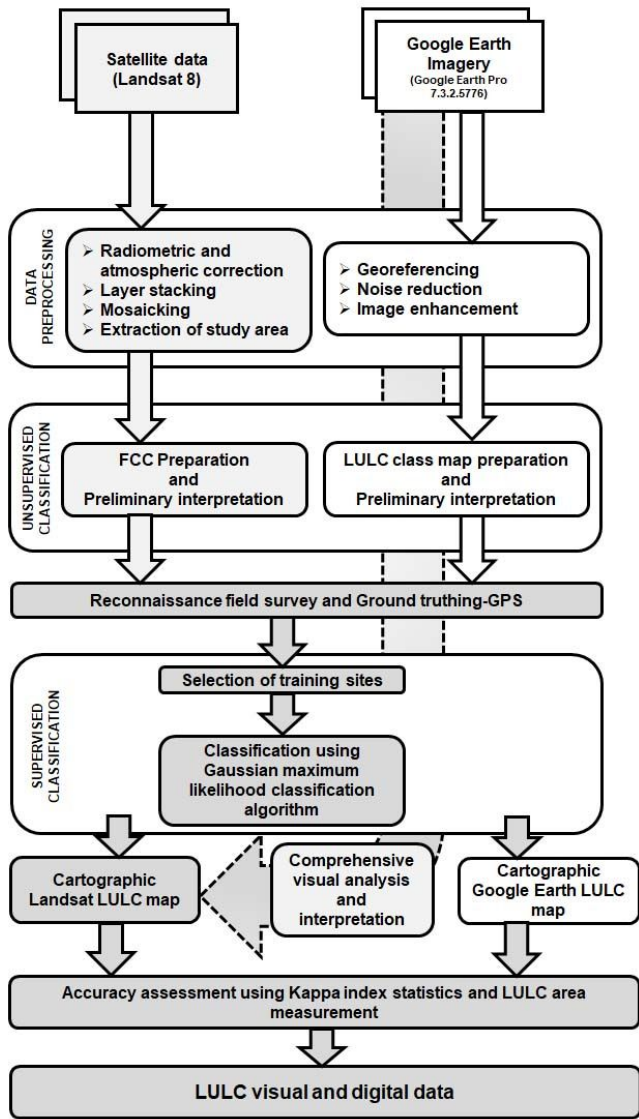


Figure 3

An overview of RS-GIS based land use land cover (LULC) analysis.

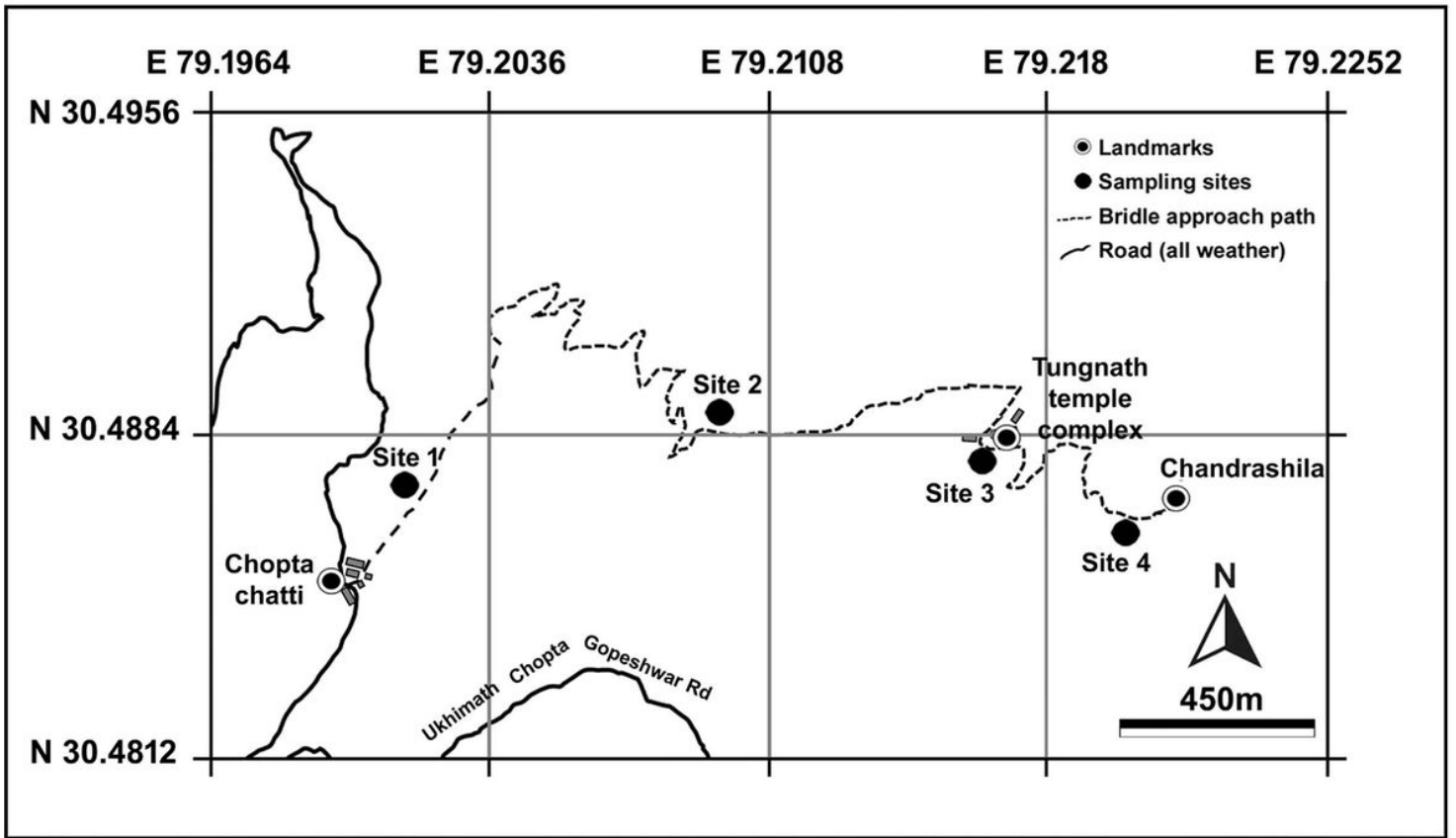


Figure 4

The detailed map of study area depicting all the sampling sites and landmarks in Chopta-Tungnath landscape.

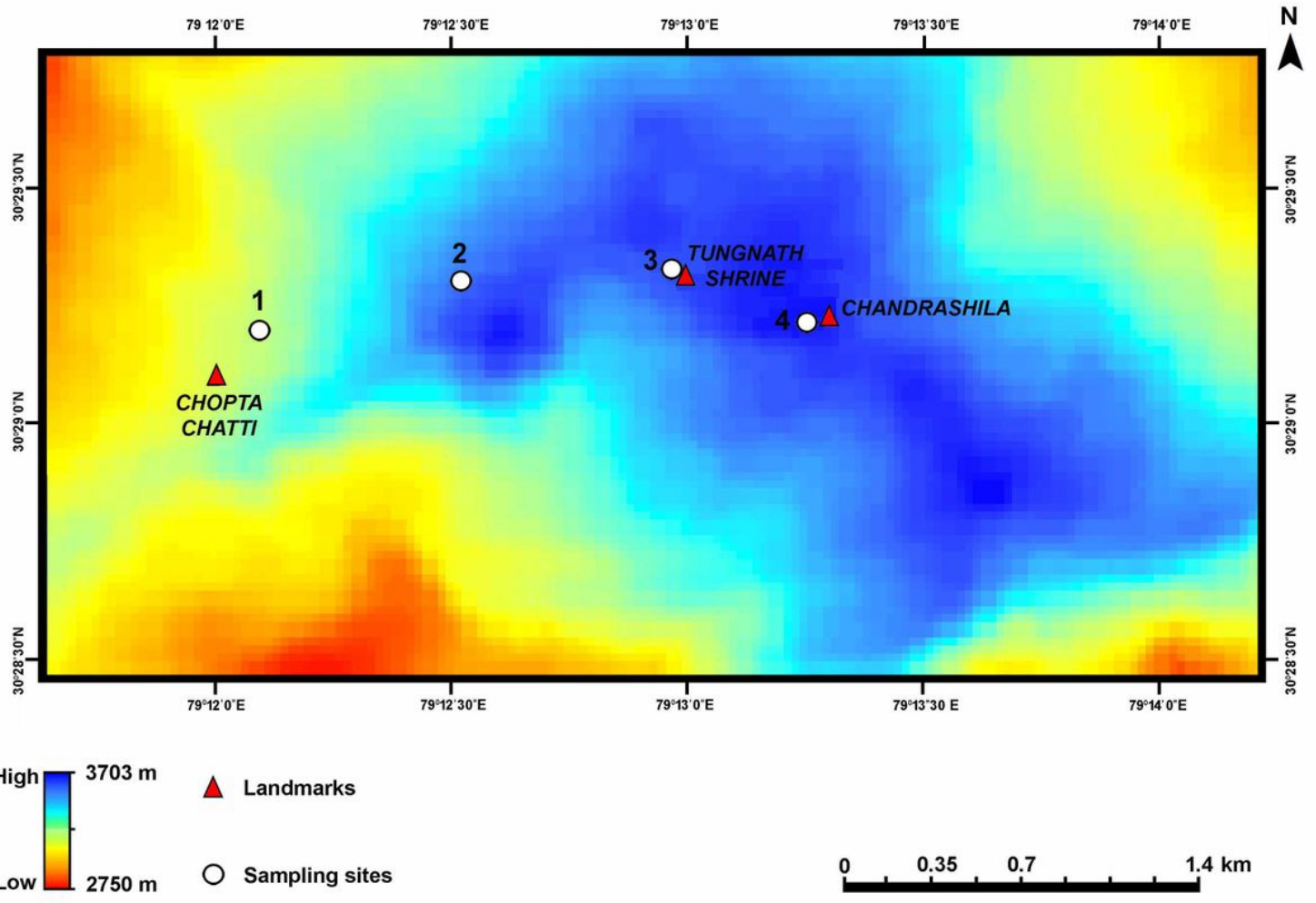


Figure 5

The SRTM-DEM visualized map with sampling sites and major landmarks tagged.

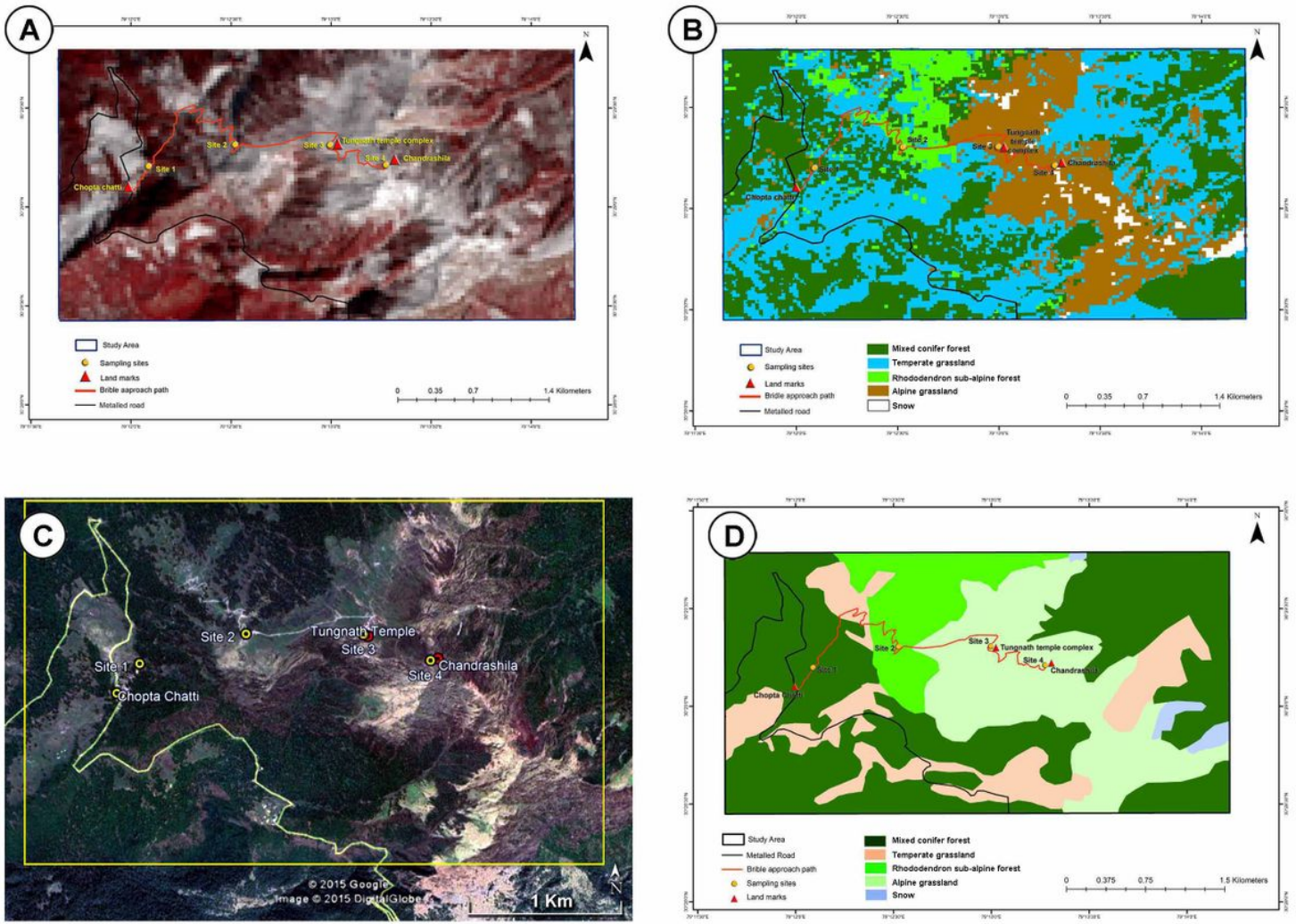


Figure 6

The RS-GIS based land use land cover (LULC) classification of the Chopta-Tungnath landscape-A, The Landsat 8, 2014 false-colour composite map of Chopta-Tungnath landscape; B, The digital supervised LULC classes of Landsat 8 data; C, The Google earth pro map of the study area; D, The visual classified LULC classes of Google earth pro map data.

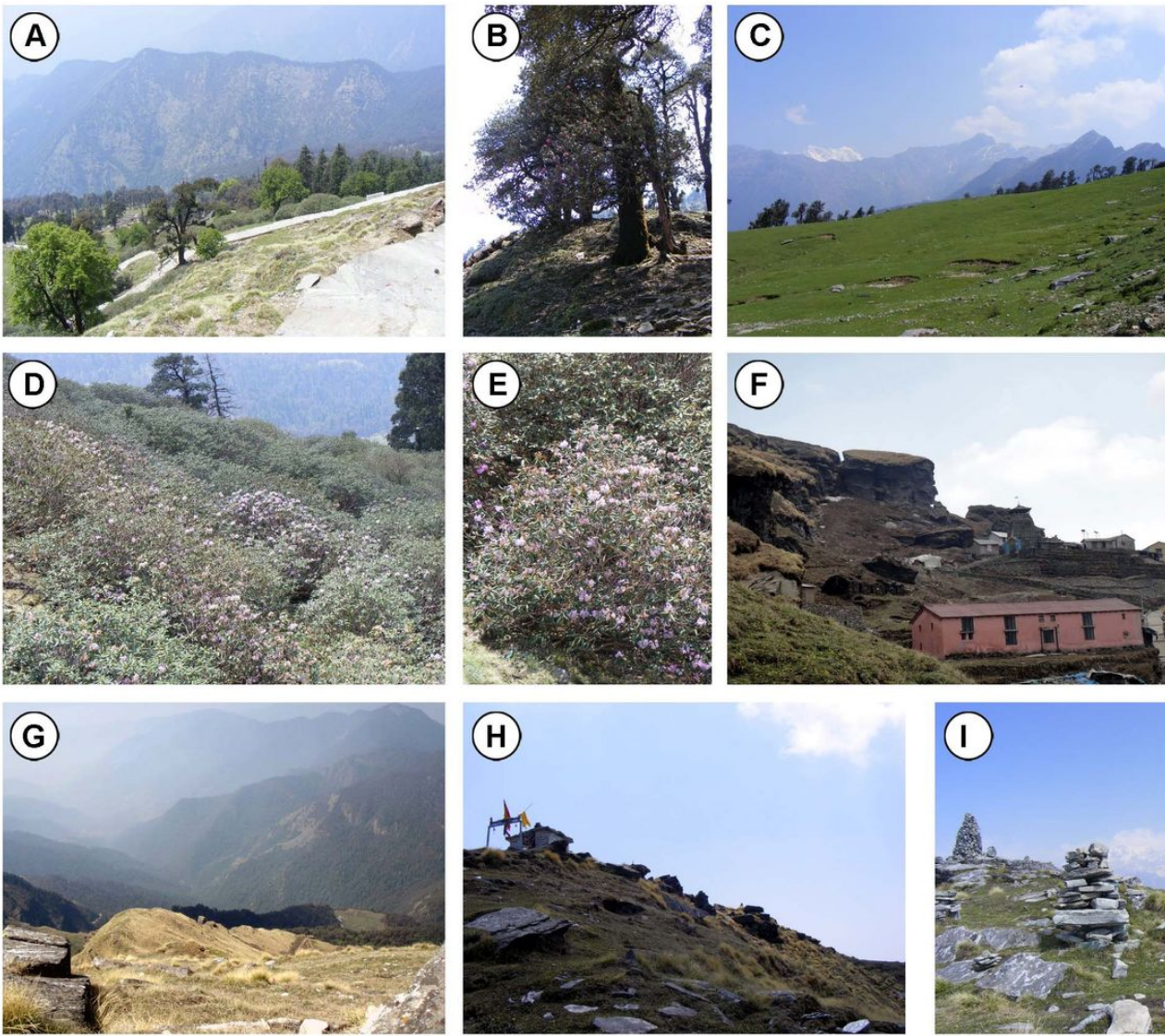


Figure 7

The environs of Chopta-Tungnath landscape-A. The mixed conifer forests; B. *Rhododendron arboreum* strand in mixed conifer forest; C, The temperate grasslands; D, The *Rhododendron* sub-alpine forest; E, *Rhododendron campanulatum* stand in *Rhododendron* sub-alpine forest; F, The Tungnath shrine; G, The alpine grassland; H, The Chandrashila; I, The cairns at Chandrashila.

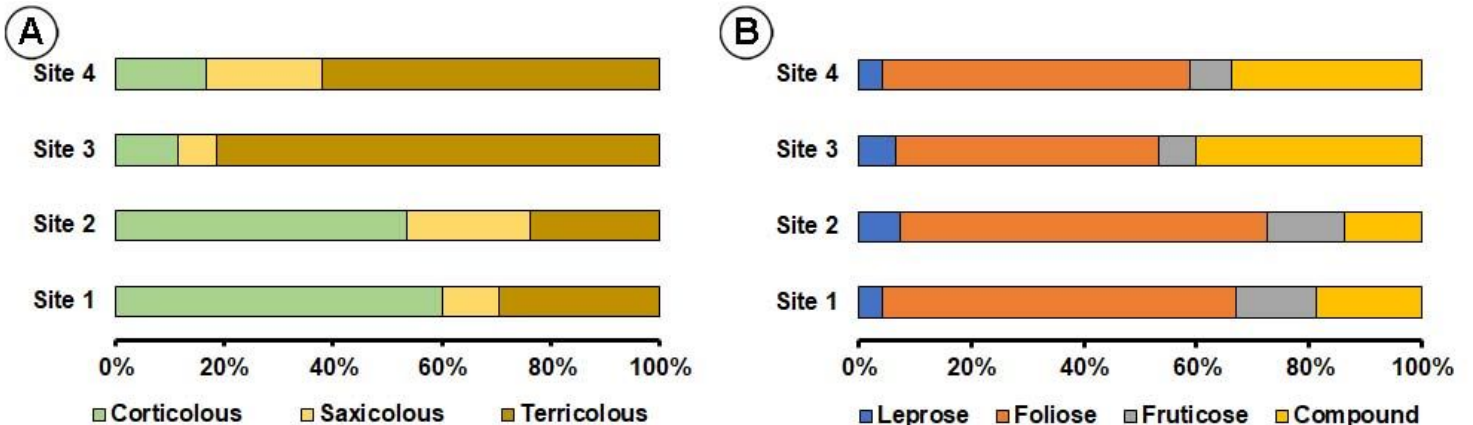


Figure 8

The site-wise variation of A, lichen habitat-subsets; B, lichen growth forms in the Chopta–Tungnath landscape.

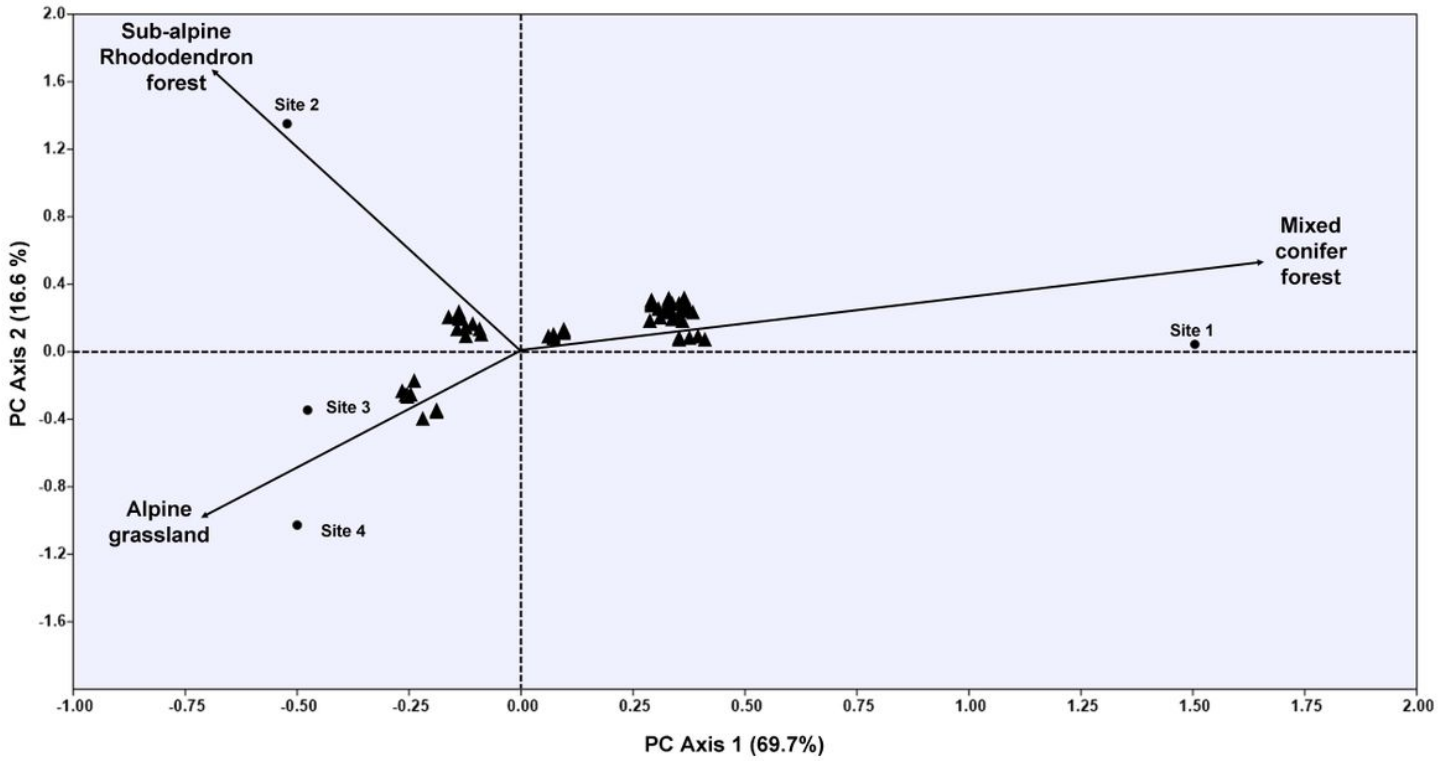


Figure 9

PCA ordination bi-plot of the four lichen study site data along the three RS-GIS recognized LULC classes in the Chopta–Tungnath landscape.